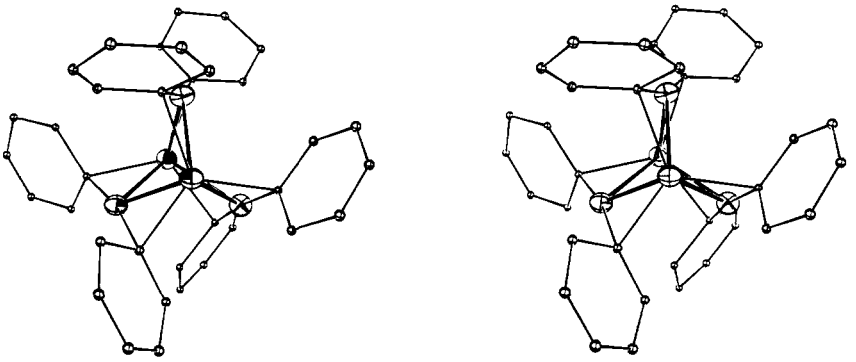

Figure 2. Stereoscopic view of the $[Cu_5Ph_6]^-$ cluster as found in the $[Li(PMDTA)(THF)]^+$ salt. This molecular plot is drawn in a different orientation from the one shown in Figure 1; however, the $[Cu_5Ph_6]^-$ clusters in the two salts are virtually identical.

rather similar to that of $[Cu_5(S\text{-}t\text{-}Bu_6)]^-$.[10]

Although many copper/aryl clusters with substituted phenyl groups are known,[11-14] this work represents, to our knowledge, the first structural characterization of a copper cluster with unsubstituted phenyl ligands. All previous structure determinations[11-14] involved bidentate aryl ligands with lone-pair-containing substituents (such as NMe_2 or OMe).[15] For the parent phenyl ligand, other known bridging structures include those of Al_2Ph_6,[16] $Al_2Ph_2Me_4$,[17] $(LiPh\cdot TMED)_2$[18] (TMED = tetramethylethylenediamine), $[Li(TMED)]_2[Mg_2Ph_6]$,[19] and the osmium cluster complex $Os_3(CO)_8(PPh_2)(Ph)(PPhC_6H_4)$.[20] In all cases, the perpendicular bridging configuration of the phenyl ring was found.[11-14,16-20]

The bonding in the copper–phenyl–copper bridge, as pointed out earlier,[13,21] is probably a combination of three-center interactions involving the two Cu atoms and the carbon sp^2 and p orbitals (i.e., I and II respectively). Interaction II is the factor

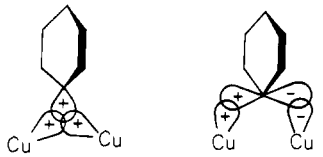

I II

most likely responsible for maintaining the phenyl group in a perpendicular orientation, while interaction I implies some degree of Cu–Cu bonding. The question of Cu–Cu interactions in Cu clusters has been discussed by Mehrotra and Hoffmann,[22] who concluded that, in many cases, weak Cu–Cu interactions exist. In $[Cu_5Ph_6]^-$, one can probably assume that the short Cu(ax)–Cu(eq) interactions are weakly bonding but that the long Cu(eq)–Cu(eq) interactions are essentially nonbonding.

Acknowledgment. We thank the National Science Foundation for supporting this work through Grants CHE-79-26479 and CHE-81-01122 and Kevin Brooks and Michael Chiang for computational assistance.

Registry No. $[Li(THF)_4]^+[Cu_5Ph_6]^-$, 81027-54-5; $[Li(PMDTA)(THF)]^+[Cu_5Ph_6]^-$, 81027-56-7.

Supplementary Material Available: Listing of the final atomic parameters for the $[Cu_5Ph_6]^-$ anion in $[Li(THF)_4]^+[Cu_5Ph_6]^-$ and in $[Li(PMDTA)(THF)]^+[Cu_5Ph_6]^-$ (2 pages). Ordering information is given on any current masthead page.

(10) Dance, I. G. *J. Chem. Soc., Chem. Commun.* **1976**, 68.
(11) (a) van Koten, G.; Noltes, J. G. *J. Organomet. Chem.* **1975**, *84*, 129. (b) Guss, J. M.; Mason, R.; Sotofte, I.; van Koten, G.; Noltes, J. G. *J. Chem. Soc., Chem. Commun.* **1972**, 446.
(12) (a) van Koten, G.; Noltes, J. G. *J. Organomet. Chem.* **1975**, *102*, 551. (b) Guss, J. M.; Mason, R.; Thomas, K. M.; van Koten, G.; Noltes, J. G. *Ibid.* **1972**, *40*, C79.
(13) ten Hoedt, R. W. M.; Noltes, J. G.; van Koten, G.; Spek, A. L. *J. Chem. Soc., Dalton Trans.* **1978**, 1800.
(14) Camus, A.; Marsich, N.; Nardin, G.; Randaccio, L. *J. Organomet. Chem.* **1979**, *174*, 121.
(15) However, the same structural features (i.e., Cu···Cu bridged distances of 2.3–2.5 Å, phenyl rings perpendicular to the Cu···Cu vector, etc.) are found in complexes of both substituted and unsubstituted phenyl ligands.
(16) (a) Malone, J. F.; McDonald, W. S. *J. Chem. Soc., Dalton Trans.* **1972**, 2646. (b) Malone, J. F.; McDonald, W. S. *Chem. Commun.* **1967**, 444.
(17) (a) Malone, J. F.; McDonald, W. S. *J. Chem. Soc., Dalton Trans.* **1972**, 2649. (b) Malone, J. F.; McDonald, W. S. *Chem. Commun.* **1970**, 280.
(18) Thoennes, D.; Weiss, E. *Chem. Ber.* **1978**, *111*, 3157.
(19) Thoennes, D.; Weiss, E. *Chem. Ber.* **1978**, *111*, 3726.
(20) Bradford, C. W.; Nyholm, R. S.; Gainsford, G. J.; Guss, J. M.; Ireland, P. R.; Mason, R. *J. Chem. Soc., Chem. Commun.* **1972**, 87.
(21) van Koten, G.; Noltes, J. G. *J. Am. Chem. Soc.* **1979**, *101*, 6593.
(22) Mehrotra, P. K.; Hoffmann, R. *Inorg. Chem.* **1978**, *17*, 2187.

Initial Fluorescence Depolarization of Tyrosines in Proteins

Ronald M. Levy*

Department of Chemistry, Rutgers, The State University New Brunswick, New Jersey 080903

Attila Szabo*

Laboratory of Chemical Physics National Institute of Arthritis, Diabetes, and Digestive and Kidney Diseases National Institutes of Health, Bethesda, Maryland 20205

Received December 21, 1981

A wide variety of experimental and theoretical techniques are providing an increasingly detailed picture of the internal dynamics of proteins.[1] This information is essential for an understanding at the molecular level of the relationship between structure and function for processes requiring protein flexibility. Both fluorescence depolarization[2,3] and ^{13}C nuclear magnetic resonance (NMR) relaxation experiments[4-6] can provide information about fast (picosecond–nanosecond) protein motions. Theoretical studies[7] using molecular dynamics computer simulation methods have

(1) M. Karplus and J. A. McCammon, *CRC Crit. Rev. Biochem.*, *9*, 293 (1981).
(2) I. Munro, I. Pecht, and L. Stryer, *Proc. Natl. Acad. Sci. U.S.A.*, *76*, 56 (1979).
(3) J. R. Lakowicz and G. Weber, *Biophys. J.*, *32*, 591 (1980).
(4) R. J. Wittebort, M. Rothgeb, A. Szabo, and F. R. N. Gurd, *Proc. Natl. Acad. Sci. U.S.A.*, *76*, 1059 (1979).
(5) R. Richarz, K. Nagayama, and K. Wüthrich, *Biochemistry*, *19*, 5189 (1980).
(6) A. Ribeiro, R. King, C. Restivo, and O. Jardetzky, *J. Am. Chem. Soc.*, *102*, 4040 (1980).
(7) J. A. McCammon and M. Karplus, *Annu. Rev. Phys. Chem.*, *31*, 29 (1980).

0002-7863/82/1504-2073$01.25/0

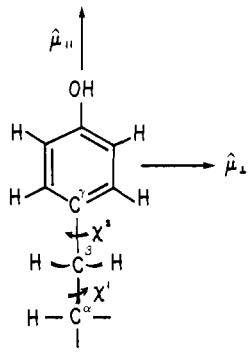

Figure 1. Structure of the tyrosine side chain. The absorption and emission dipoles are assumed to be coincident. Calculations were performed with the absorption dipole parallel ($\hat{\mu}_{\parallel}$) and perpendicular ($\hat{\mu}_{\perp}$) to the C^{β}–C^{γ} axis.

demonstrated that significant atomic fluctuations occur in the protein interior on a picosecond time scale. In a recent communication,[8] the effects of these picosecond protein fluctuations on the NMR spin lattice T_1's of selected protonated carbons in pancreatic trypsin inhibitor (PTI) were considered. It was shown that the picosecond motional averaging of the CH dipole vector can increase T_1 by 10–100%. Here we consider the implications of this study for the time-resolved fluorescence emission anisotropy of tyrosines (Tyr) in PTI by exploiting the formal correspondence[9] between dipolar NMR relaxation and fluorescence depolarization. Both the measured NMR dipolar relaxation and the fluorescence depolarization parameters depend on time-correlation functions of the reorienting probe vectors. NMR relaxation rates are determined by Fourier transforms of these time-correlation functions, the spectral densities that are functions of both the fast protein motions and the much slower protein tumbling. The fluorescence depolarization, however, depends directly on the decay of the time-correlation functions so that the initial rate of decay of the emission anisotropy reflects only the fast protein motions. We used a 96-ps molecular dynamics simulation[10] of PTI at 300 K to investigate the influence of picosecond motions of tyrosines on their extrapolated initial fluorescence depolarization.

The time resolved fluorescence emission anisotropy of a fluorophore in an isotropically reorienting protein is

$$r(t) = {}^2/_5 e^{-t/\tau_M}\langle P_2(\mu_a(0)\cdot\mu_e(t))\rangle \qquad (1)$$

where τ_M is the correlation time for the overall motion of the protein, $P_2(x)$ is the second Legendre polynomial and μ_a and μ_e are unit vectors pointing along the absorption and emission dipoles, respectively. The emission anisotropy at zero time is

$$r(0) = 0.4P_2(\cos\delta) \qquad (2)$$

where δ is the angle between μ_a and μ_e. When these vectors coincide ($\delta = 0$), $r(0) = 0.4$. In this case eq 1 becomes

$$r(t) = {}^2/_5 e^{-t/\tau_M}\langle P_2(\mu(0)\cdot\mu(t))\rangle = \frac{8\pi}{25} e^{-t/\tau_M} \sum_{m=-2}^{2} \langle Y_{2m}^*(\Omega(0)) Y_{2m}(\Omega(t))\rangle \qquad (3)$$

where we have used the addition theorem for spherical harmonics.[11] The polar angles $\Omega \equiv (\theta,\phi)$ specify the orientation of μ in a macromolecule-fixed frame. Using the 96-ps molecular dynamics trajectory,[10] we have evaluated the correlation functions in eq 3 for the four tyrosine rings in PTI. For illustrative purposes, we chose two different oritentations of the emission (absorption) dipole as shown in Figure 1. To a good approximation $r(t)$ decays to a plateau value in about 2 ps. The plateau value of the correlation function describing the internal motions is equal to the generalized order parameter,[12,13] $\mathcal{S}^2$, which is given by

$$\mathcal{S}^2 = \frac{4\pi}{5}\sum_{m=-2}^{2} |\langle Y_{2m}(\Omega)\rangle|^2 = \frac{4\pi}{5}\sum_{m=-2}^{2}\left|\frac{1}{T}\int_0^T Y_{2m}(\Omega(t))\,dt\right|^2 \qquad T = 96 \text{ ps} \quad (4)$$

where we have replaced the ensemble average by the time average. The generalized order parameter satisfies $0 \le \mathcal{S}^2 \le 1$ and is a measure of the spatial restriction of the motion in the sense that $\mathcal{S} = 0$ when the motion is isotropic while $\mathcal{S} = 1$ if it is completely restricted. Using the above results, we can write

$$r(t)/r(0) = \mathcal{S}^2 e^{-t/\tau_M} \qquad t > 2 \text{ ps} \qquad (5)$$

Thus, if the resolution of a fluorescence depolarization experiment is less than 2 ps as a result of the finite width of the excitation pulse, eq 5 shows that $r(t)$ decays with a correlation time corresponding to the overall motion of the protein, but the extrapolated value of the anisotropy at zero time, $r_e(0)$ is anomalously low ($r_e(0) = r(0)\mathcal{S}^2$).

In Table I we present values of $r(2\,\text{ps})/r(0)$ for the tyrosine resides of PTI along with the values of $\mathcal{S}^2$ calculated from eq 4. The close agreement between the two quantities is a reflection of the fact that the correlation function describing internal motions does not significantly decay further after 2 ps. With the exception of Tyr 10, the results show that the extrapolated initial anisotropy is about 7–19% smaller than the theoretical limit that would be realized in the absence of internal motions (i.e., in the limit of very low temperatures). Tyr 10 undergoes larger amplitude motion; Tyr 10 is close to the protein surface so that the ring motions are expected to be somewhat less restricted. Although the exact dynamics of aromatic ring motions in proteins are quite complex, it may still be useful to interpret the time-resolved fluorescence depolarization in terms of simple models for the motion. For the model where the fluorophore absorption dipole moves freely within a cone of semiangle α_0, the cone semiangle can be related to the probe order parameter.[9] For the order parameters listed in Table I, the cone semiangle, α_0, is approximately 15–35°.

Table I. Fluorescence Depolarization of Tyrosines at t = 2 ps for Two Orientations of the Emission (Absorption) Dipole Shown in Figure 1[a]

residue	$\mu_{\parallel}$, $r(2\text{ ps})/r(0)$	$\mu_{\perp}$, $r(2\text{ ps})/r(0)$
Tyr 10	0.88 (0.86)	0.64 (0.58)
Tyr 21	0.93 (0.91)	0.89 (0.87)
Tyr 23	0.92 (0.91)	0.85 (0.85)
Tyr 35	0.88 (0.86)	0.84 (0.81)

[a] The value of the generalized order parameter, $\mathcal{S}^2$, for internal motions calculated by using eq 4 is given in parentheses.

The time-resolved fluorescence depolarization of tryptophan residues has been measured in a variety of proteins.[2,3] Munro et al.[2] fitted the time dependence of the decay to a sum of two exponentials and interpreted their results by using the wobbling in a cone model. The reported cone semiangles for tryptophan wobbling are comparable to values calculated for the tyrosines of PTI by using the molecular dynamics trajectory, but the time constant for the motion is at least 2 orders of magnitude slower than the picosecond plateau times for the tyrosine rings in PTI. While it is possible that the increased bulk of the tryptophan side chain is associated with slower wobbling, a careful analysis of the extrapolated initial fluorescence depolarization is required in order to evaluate the effect of picosecond tryptophan motions on the fluorescence depolarization. For the five single tryptophan proteins studied by Munro et al.[2] the extrapolated initial fluorescence anisotropies varied between 0.18 and 0.26. The low values (<0.4)

(8) R. M. Levy, M. Karplus, and J. A. McCammon, *J. Am. Chem. Soc.*, *103*, 994 (1981).
(9) G. Lipari and A. Szabo, *Biophys. J.*, *30*, 489 (1980).
(10) M. Karplus and J. A. McCammon, *Nature (London)*, *277*, 578 (1979).
(11) D. M. Brink and G. R. Satchler, "Angular Momentum", 2nd ed., Clarendon Press, Oxford, England, 1961.
(12) G. Lipari and A. Szabo, *J. Am. Chem. Soc.*, in press.
(13) R. M. Levy, C. Dobson, and M. Karplus, *Biophys. J.*, in press.

result in part from the fact that the emission and absorption dipoles are not parallel ($\delta \neq 0$). It is possible, however, that the variation in initial values observed reflects differences in mobility among these fluorophores on the picosecond time scale. It is of interest to note that while Munro et al. concluded the tryptophan of Staphylococcus aureus nuclease B is rigid, it had the smallest initial anisotropy (0.18) of the five proteins studied. A similar anomalously low value of $r_e(0) = 0.18$ has been reported for the tryptophans in carbonic anhydrase. Lakowicz and Weber[3] suggest subnanosecond tryptophan motions may be responsible for this small initial fluorescence depolarization. Measurements of fluorescence depolarization of tyrosines in proteins would be of interest both for comparison with experimental results already obtained for the bulkier tryptophan residues and for comparison with the values calculated for the initial fluorescence depolarization of tyrosines obtained from a molecular dynamics simulation. Such measurements on tyrosines in PTI are in progress.[14]

Acknowledgment. We are grateful to M. Karplus for providing the PTI molecular dynamics trajectory. R.M.L. acknowledges support from the Rtugers University Research Council, BRSG, and the donors of the Petroleum Research Fund, administered by the American Chemical Society.

Registry No. PTI, 50936-63-5.

(14) A. Kasprzak and G. Weber, to be submitted for publication.

The Use of "Enantiopolar" Directions in Centrosymmetric Crystals for Direct Assignment of Absolute Configuration of Chiral Molecules: Application to the System Serine/Threonine

L. Addadi,* Z. Berkovitch-Yellin,* I. Weissbuch,* M. Lahav,* and L. Leiserowitz*

Department of Structural Chemistry The Weizmann Institute of Science Rehovot 76100, Israel

S. Weinstein*

Department of Organic Chemistry The Weizmann Institute of Science Rehovot 76100, Israel

Received August 31, 1981

X-ray analysis does not distinguish between enantiomeric crystal structures $\{R\}_d$ and $\{S\}_l$ [where the enantiomerically resolved molecules R and S pack in the corresponding $\{\}_d$ and $\{\}_l$ chiral crystal] unless the Bijvoet method of anomalous dispersion is applied. On the other hand, X-ray analysis of a centrosymmetric crystal composed of a racemate $\{RS\}$ establishes unambiguously the sites occupied by the R and S moieties with respect to the crystal axes (Figure 1). Consequently, in contradistinction to chiral crystals, the orientation toward all crystal faces of the substituents attached to the R and S chiral molecules is unambiguously assigned.[1] However, because of the coexistence of the two enantiomers in the crystals, this knowledge cannot be directly exploited for the assignment of absolute configuration of chiral resolved molecules. This limitation may be circumvented if the structural information contained in the racemic crystal is transferred to a third chiral molecule, interacting stereospecifically with the racemic system through a well-defined mechanism.

Our studies on inhibition of growth of conglomerates[2] and polar crystals[1] by adsorption of resolved "tailor-made" impurities have led to an understanding of the correlation between the crystal structure of the substrate, molecular structure of the additive, and the affected growth directions, as revealed by specific morphological changes. This correlation has been applied for a direct assignment of the absolute configuration of chiral polar crystals.[1] The same approach is adopted here for the direct assignment of absolute configuration of resolved impurities through morphological changes induced stereoselectively on the enantiotopic faces of centrosymmetric crystals with appropriate packing features. A requirement for application of this method is that within the racemic crystal specific functional groups attached to an R molecule (Scheme I) point toward faces hkl (f1), but not toward $\bar{h}\bar{k}\bar{l}$ (f$\bar{1}$), while the same functional groups attached to an S molecule will emerge at the enantiotopic faces $\bar{h}\bar{k}l$, but not toward hkl.

Let us consider the crystallization of a racemate of this type, in the presence of a chiral additive R', appropriately designed so that it will fit in the site of an R molecule on the growing crystal faces f1 or f2 (Scheme I) but not at the enantiotopic faces f$\bar{1}$ or f$\bar{2}$. On the basis of the above mechanism of inhibition previously investigated,[1,2] this adsorbed molecule will hinder growth along the $+b$ direction but not along $-b$. It is therefore expected that either the areas of the f1 and f2 faces will increase relative to their enantiotopic faces or new faces will appear on the $+b$ side of the crystal. By virtue of symmetry, additive S' will inhibit growth of faces f$\bar{1}$ and f$\bar{2}$, but not f1 and f2, while racemic $R'S'$ will inhibit

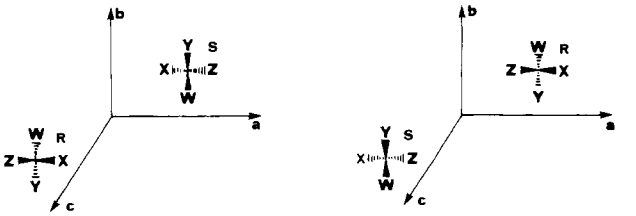

Figure 1. On the left, chiral molecules R and S are related by a center of inversion at the origin; interchanging them leads to the diastereomeric arrangement shown on the right. Therefore the orientation of groups w, x, y, z of one chirality in a given crystal structure is unambiguously fixed with respect to the a, b, c axes.

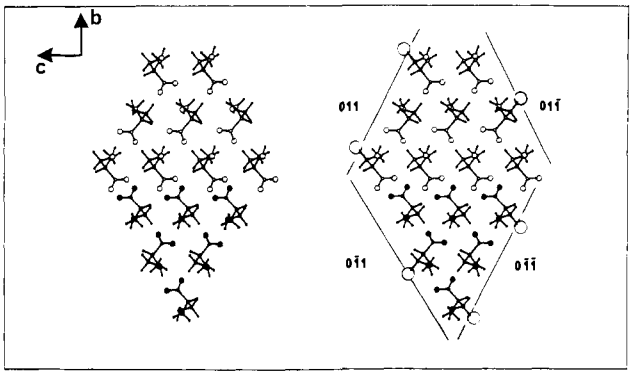

Figure 2. Packing of $\{RS\}$-serine viewed along the a axis. Molecules are packed in b c layers which are homochiral. For clarity only half of each R (open circles) and S (full circles) layer is shown. The four {011} crystal faces are shown. Threonine impurity molecules (with the $-CH_3$ group indicated by large circles), are inserted stereospecifically.

Scheme I

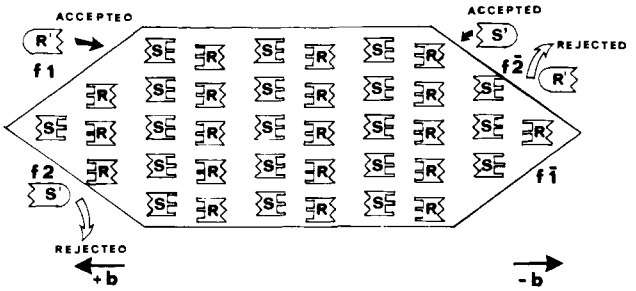

(1) For part 2, see Z. Berkovitch-Yellin, L. Addadi, M. Idelson, L. Leiserowitz, and M. Lahav, *Nature (London)*, in press.

(2) L. Addadi, Z. Berkovitch-Yellin, N. Domb, E. Gati, M. Lahav, and L. Leiserowitz, *Nature (London)*, in press.

0002-7863/82/1504-2075$01.25/0